The Effects of Tides and Oscillatory Winds on the Subtidal Inner-Shelf Cross-Shelf Circulation

RENATO CASTELAO

Department of Marine Sciences, The University of Georgia, Athens, Georgia

ROBERT CHANT, SCOTT GLENN, AND OSCAR SCHOFIELD

Institute of Marine and Coastal Sciences, Rutgers, The State University of New Jersey, New Brunswick, New Jersey

(Manuscript received 20 April 2009, in final form 4 September 2009)

ABSTRACT

A two-dimensional numerical model is used to investigate the effects of tidal forcing and oscillatory winds on the subtidal cross-shelf circulation on the inner shelf. Bottom topography and initial stratification are representative of the South and Middle Atlantic Bights along the U.S. east coast. Results from simulations forced by upwelling winds and no tides are consistent with previous studies of inner-shelf circulation. The inclusion of tidal forcing leads to increased mixing, larger eddy viscosity coefficients, and reduced stratification over the shallow regions, effectively reducing the wind efficiency to drive cross-shelf currents on the inner shelf. Tidally averaged cross-shelf currents are weaker compared to when no tides are considered. There is an increase in the width of the region of surface wind-driven transport divergence, which changes the cross-shelf location where upwelling occurs. Lagrangian analyses indicate that tidal forcing substantially reduces the transport of offshore waters toward the coast and increases the residence time over the inner shelf by up to 70%. Fluctuating winds with zero mean lead to a rectification of the cross-shelf flow on the inner shelf, resulting in net upwelling. The rectification occurs because the cross-shelf transport is nonzero during upwelling wind forcing (since dense water is brought to the inner shelf maintaining the stratification), but is approximately zero during downwelling winds (since surface water is forced under near-bottom water, destroying the stratification). The rectification is more clearly observed when stratification is strong, when tidal forcing is weak or absent, and when the wind fluctuates at low frequency.

1. Introduction

Wind-driven cross-shelf currents play an important role in the transport of heat, salt, nutrients, detritus, phytoplankton, sediments, pollutants, and larvae on most continental shelves. They are also an important component of the upwelling circulation that typically brings cold, nutrient-rich subsurface waters to the surface, fueling phytoplankton growth and influencing the water column density structure. The cross-shelf circulation associated with alongshelf winds has been well documented for wind-driven middle and outer shelves with small alongshelf topographic variability, being characterized by a surface Ekman transport that is compensated by a return flow that exists either in the interior of the fluid or in a bottom boundary layer (e.g., Allen 1980; Huyer 1990; Smith 1995; Lentz and Chapman 2004, among others).

At the inner continental shelf, however, offshore of the surf zone where the surface and bottom boundary layers interact, the mechanisms that drive cross-shelf flow are much less understood, having only recently become an active area of research. Previous studies have shown that the cross-shelf circulation driven by alongshelf winds in this shallow area depends strongly on vertical mixing (Lentz 1995) and stratification (Lentz 2001; Austin and Lentz 2002; Kirincich et al. 2005). During unstratified periods, the increased turbulence throughout the water column leads to increased boundary layer thickness (δ_E) (Ekman 1905). For water depths h of order δ_E or less, the surface and bottom Ekman layers interact and the transport perpendicular to the applied stress is reduced until the transport is entirely downwind for water depths much less than δ_E. A divergence in the wind-driven cross-shelf

Corresponding author address: Renato Castelao, Dept. of Marine Sciences, The University of Georgia, Marine Sciences Bldg., Athens, GA 30602.
E-mail: castelao@uga.edu

DOI: 10.1175/2009JPO4273.1

transport is established between the coast, where the transport is zero (no flow across the boundary), and deep waters ($h >> \delta_E$), where the transport approaches the theoretical Ekman value. Using mooring observations from the North Carolina shelf, Lentz (2001) showed that the width of the region of reduced cross-shelf transport (compared to the theoretical Ekman transport) during the unstratified season can be very large, often extending all the way to the shelf break.

If stratification is significant, however, vertical mixing is reduced, leading to thinner boundary layers. This allows the wind-driven cross-shelf circulation to extend into shallower water compared to the unstratified case (Allen et al. 1995; Lentz 2001). Austin and Lentz (2002) used a two-dimensional numerical model to show that, for a stratified shelf under upwelling-favorable winds, the onshore return flow at depth that compensates the surface Ekman transport brings denser water all the way to the inner shelf, maintaining a weak stratification. They showed that this weak stratification is enough to reduce vertical mixing and the stress in the midwater column, allowing for a cross-shelf circulation to be established. Off the North Carolina coast, for example, cross-shelf circulation exists within a few kilometers of the coast during the stratified season (Lentz 2001).

Austin and Lentz's (2002) results also reveal that the situation during downwelling-favorable wind forcing is quite different. The cross-shelf circulation induced by downwelling winds in an initially stratified shelf forces surface, light water under near-bottom, denser waters. This leads to convection, substantially increasing the mixing and decreasing the stratification. As a consequence of the reduced stratification, the cross-shelf circulation at the inner shelf is virtually shutdown, being substantially weaker than when winds are upwelling favorable. The response of the inner-shelf circulation to upwelling and downwelling wind forcing is, therefore, asymmetric.

The majority of the previous investigations of wind-driven cross-shelf currents over the inner shelf did not address directly the effects of tides on the circulation. Tidal currents can have an important impact on the strength and structure of the stratification, particularly over the shallower regions close to the coast. Studies from the mid-1970s have shown marked frontal structures occurring on the European continental shelf during summer associated with variations in the level of tidal mixing. Their locations are essentially determined by the ratio of the water depth and the cube of the amplitude of the tidal currents (Simpson and Hunter 1974; Simpson et al. 1978; Garrett et al. 1978; Limeburner and Beardsley 1982; He and Wilkin 2006; Wilkin 2006, among others). These studies indicate that, if the water depth is small (as in the inner shelf) and the tidal currents amplitude is large enough, tidal stirring can be sufficiently strong to vertically mix the water column. Even if the water column is not completely mixed, tidal stirring can substantially reduce the stratification near the coast. Since stratification has been shown to substantially affect the wind-driven cross-shelf circulation over the inner shelf, there is the potential for tides to affect the *wind-driven* inner-shelf cross-shelf currents.

In this manuscript, we use a numerical model to address directly the effects of tides and oscillatory winds on the subtidal inner-shelf cross-shelf circulation. In particular, we investigate if tides, by changing the stratification, can affect the divergence in the surface wind-driven transport, from zero at the coast to the full Ekman transport at midshelf. We also investigate the importance of the asymmetric response of the inner shelf to upwelling–downwelling wind forcing and the net effect of oscillatory winds with zero mean on the cross-shelf currents. Changes in the subtidal inner-shelf cross-shelf circulation have important ecosystem implications, since they can lead to changes in the supply of cold, nutrient-rich waters to the regions close to the coast. Our model implementation is representative of conditions along the U.S. east coast, a region where tidal currents are generally significant (e.g., Battisti and Clarke 1982).

2. Methods

The Regional Ocean Modeling System (ROMS) used here is a free-surface, hydrostatic, primitive equation numerical circulation model with terrain-following vertical coordinates that is described in detail by Shchepetkin and McWilliams (2005) and Haidvogel et al. (2008). For this study, the only prognostic scalar variable calculated is potential density. The advection scheme utilized is the third-order upwind scheme of Shchepetkin and McWilliams (1998). The model incorporates the Mellor and Yamada (1982) 2.5-level turbulence closure scheme as modified in Galperin et al. (1988). The pressure gradient scheme is a spline density Jacobian (Shchepetkin and McWilliams 2003), which minimizes the errors associated with computing horizontal pressure gradients with terrain-following coordinates.

The model domain is an across-shelf (x, z) section bounded by a vertical wall at the coast, with no variations in the alongshelf (y) direction. Although two-dimensional simulations present its limitations, it has been used recently several times with great success in inner-shelf studies (e.g., Austin and Lentz 2002; Kuebel Cervantes et al. 2003; Tilburg 2003; Lentz and Chapman 2004), and has the advantage of avoiding any questions of an artificial alongshore pressure gradient setup by

imperfect open boundary conditions. The model domain extends 120 km offshore. The grid resolution is 200 m near the coast, increasing linearly to approximately 1 km at 88 km from the coast. Offshore of that, the grid resolution remains constant. In the vertical, 40 s levels, where s denotes a generalized vertical coordinate, are utilized with grid spacing that varies so that there is higher resolution both near the surface and the bottom in order to resolve the respective boundary layers. The horizontal velocity $\mathbf{v}$ has components (u, v) corresponding to the cross- and alongshelf velocities in the (x, y) directions, so that u is positive offshore and v is positive toward the north.

The topography in the basic case is given by $h = h_0 + \alpha x$, where $h_0 = 5$ m is the depth at the coast and $\alpha = 0.001$ is the bottom slope. This is similar to the configuration used by Austin and Lentz (2002), with the exception that they used a symmetric channel so that they could investigate the upwelling and downwelling responses at the same time. That is not possible in the present study, since tidal forcing is applied at the offshore boundary (see below). This is also similar to the setup used by Tilburg (2003) and Lentz and Chapman (2004). The importance of the bottom slope in the circulation is explored by using a different α in a few simulations. The initial stratification in the basic case is constant, with $N = N_0 = (-g/\rho_0\, \partial\rho/\partial z)^{1/2} = 0.0175\ s^{-1}$, where N is the buoyancy frequency, g is the gravitational acceleration, ρ is the density, ρ_0 is a reference density, and z is the vertical coordinate. A few simulations were also initialized with $N = 0.5N_0$ and $N = 1.5N_0$, so that the effects of the strength of the stratification could be explored. The stratification in the basic case is somewhat weaker, but similar, to the values used by Tilburg (2003) and by Austin and Lentz (2002) in their constant-stratification case. It is also within the range of the constant stratifications used by Lentz and Chapman (2004). The relevance of using initial constant stratification is addressed in the discussion section. For the combination of bottom slopes and stratifications used, the Burger number $\mathrm{Bu} = \alpha N/f$, where f is the Coriolis parameter, varied from 0.05 to 0.3, in the range of conditions commonly found on the Middle Atlantic Bight (Tilburg 2003).

At the offshore boundary, the surface elevation satisfies an implicit gravity wave radiation condition (Chapman 1985), while the depth-averaged velocities satisfy a Flather radiation scheme (Flather 1976). The values needed in the Flather scheme are specified as to impose M_2 tides in the model via the open boundary condition, and are based on Battisti and Clarke (1982). We force the model using three different scenarios, with the barotropic M_2 tidal currents' semimajor axes equal to 0.13, 0.195, and 0.26 m s^{-1}. Those values are representative of typical tidal currents observed on the Middle Atlantic Bight and the South Atlantic Bight along the U.S. east coast (Battisti and Clarke 1982). We will refer to these cases as weak, moderate, and strong tides. We also run simulations forced by the wind only. A radiation condition (Marchesiello et al. 2001) is used for the depth-dependent velocities, while we use a zero-gradient condition for density.

In the simulations intended to explore the effects of tidal forcing on the cross-shelf circulation, the model is forced by winds that are constant in time, after being ramped up over two tidal cycles. In those experiments, the alongshelf component of the wind stress is upwelling favorable at 0.1 Pa, similar to previous inner-shelf modeling studies. In other simulations, winds are defined as a cosine function, also with an amplitude of 0.1 Pa. Several different periods are used, ranging from 1 to 10 inertial periods (IP $= 2\pi/f = 18.8$ h).

To further assess the response of the inner-shelf circulation to the forcing, we define a Lagrangian label field that is advected by the model velocity, as in Kuebel Cervantes et al. (2003) and Kuebel Cervantes and Allen (2006). The label satisfies

$$\frac{DX(x,z,t)}{Dt} = 0, \tag{1}$$

where

$$\frac{D}{Dt} = \frac{\partial}{\partial t} + u\frac{\partial}{\partial x} + w\frac{\partial}{\partial z}$$

and $X(x, z, t = 0) = x$. Differencing the initial and final values at a given location gives the displacement of the water parcel. Note that the upstream bias advection scheme used in ROMS carries with it some intrinsic smoothing, introducing a small error in the Lagrangian label computation. Offshore transport in the surface layer (e.g., Table 1) is computed by integrating the cross-shelf velocities from the surface to the first zero crossing, as in Lentz (2001).

3. Results

a. Tidal forcing

The cross-shelf circulation developed in response to upwelling-favorable winds constant in time and no tides is consistent with classical coastal upwelling (Smith 1995; Allen et al. 1995). The response is unsteady (as in Allen et al. 1995; Austin and Lentz 2002; Lentz and Chapman 2004) and characterized by offshore-directed flow at the surface and onshore flow at depth, feeding an upwelling circulation. As heavier water is advected onshore and vertically, the depth-averaged water density

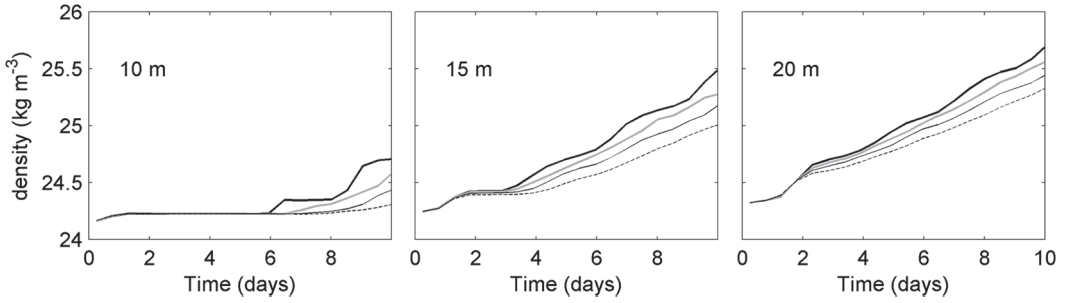

FIG. 1. Time series of tidally and depth-averaged densities at (a) 10-, (b) 15-, and (c) 20-m isobaths for simulations forced by upwelling winds only (thick black) and by winds and weak (gray), moderate (thin black), and strong (dashed) tides.

at the inner shelf increases with time (Fig. 1, thick black lines). The increase is first observed in the outer part of the inner shelf (see 20-m isobath results in Fig. 1) and is progressively observed closer to the coast. Very near the coast, at the 10-m isobath, the response in the beginning is very small, since the initial effects of the wind in these shallow waters are to increase the mixing and decrease the stratification, which leads to no significant change in the depth-average water density. After a few days, however, as dense waters are brought close to the coast by the upwelling circulation, the depth-averaged density increases rapidly. The inclusion of tidal forcing on the simulations does not change the qualitative picture described above (Fig. 1, gray, thin black, and dashed lines). However, the quantitative details of the process are modified. As the tidal current forcing increases from weak to strong, it takes longer for the same depth-averaged density to be achieved at the inner shelf.

At the 10-m isobath, the surface and bottom boundary layers overlay and the eddy viscosity is maximum in the middle of the water column in the simulation forced by no tides (Fig. 2). Farther offshore (e.g., 20-m isobath), the stratification in the interior inhibits vertical mixing, and the eddy viscosity profile presents a local minimum at middepth. The profile at the 15-m isobath indicates that is a transition region. The inclusion of tides in the simulation leads to larger eddy viscosity coefficients, consistently with the lower Richardson numbers observed in those cases (not shown). The relationship is monotonic; that is, stronger tides lead to larger coefficients. The tidal influence on the viscosity profile is more notable along the outer parts of the inner shelf (15- and 20-m isobaths in Fig. 2), where the coefficients at middepth increase by 20%–40%, 55%–80%, and 90%–130% for weak, moderate, and strong tides, respectively. This is because the water column at the 10-m isobath becomes weakly stratified very rapidly, even when the simulation is forced by winds only. After sometime, however, as the upwelling winds bring denser water toward the coast (see Fig. 1, left) and stratification develops at the 10-m isobath, the tidal influence on the eddy viscosity profile becomes more significant (not shown).

The variability in the eddy viscosity profile observed between the simulations with and without tidal forcing has important dynamical implications. Lentz (1995) showed that the location and width of the cross-shelf divergence in the Ekman transport over the inner shelf depends on the eddy viscosity profile. The vertical profile of cross-shelf velocity after 3.4 days for the simulation forced with no tides indicates that magnitudes are smaller close

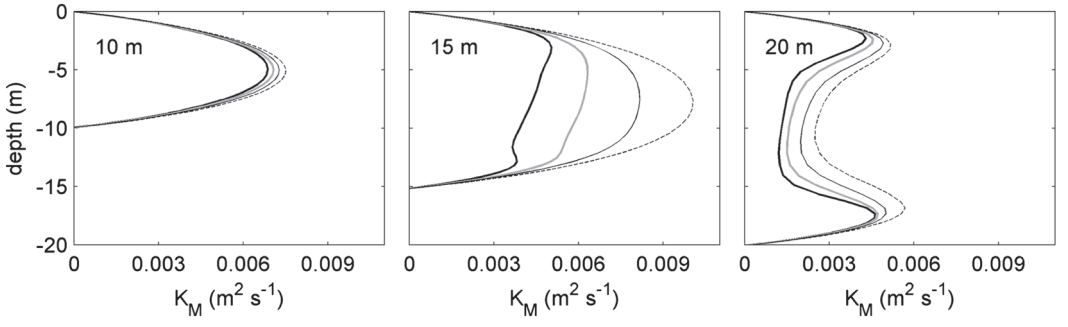

FIG. 2. Eddy viscosity profile at the (a) 10-, (b) 15-, and (c) 20-m isobaths for simulations forced by upwelling winds only (thick black) and by winds and weak (gray), moderate (thin black), and strong (dashed) tides. Values are averaged over one tidal cycle centered on day 3.36.

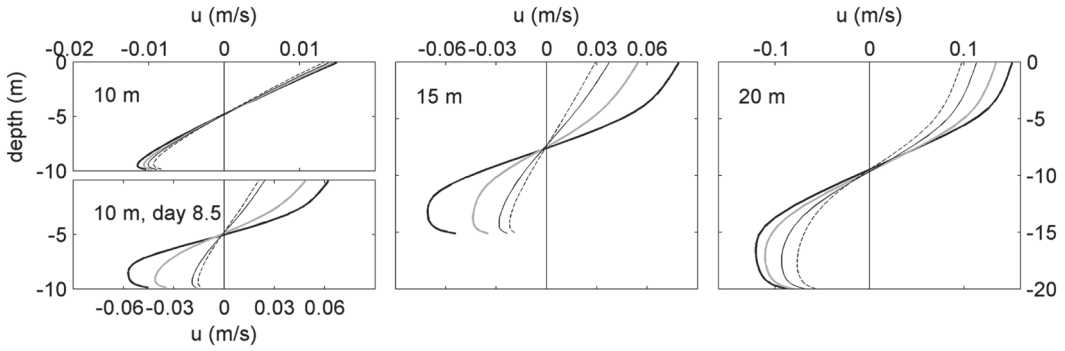

FIG. 3. Same as in Fig. 2 but for the cross-shelf velocity profile. (bottom left) Results at the 10-m isobath averaged over one tidal cycle centered on day 8.54. Note that the x axis varies between the different panels.

to the coast (where the eddy viscosity is high throughout the water column) compared to farther offshore (where the eddy viscosity presents a minimum at middepth) (Fig. 3, thick line). The inclusion of tides in the simulation substantially affects the results. There is a significant reduction in the intensity of the tidally averaged cross-shelf circulation along the inner shelf as the tidal currents increase. The decrease in the cross-shelf transport at the 10–20-m isobath is linearly related to weak/moderate increases in the eddy viscosity at midwater, with a tendency for leveling off for large increases in the eddy viscosity (Fig. 4). Note that after 8.5 days, cross-shelf currents at the 10-m isobath are still small in the moderate and strong tidal forcing cases, but have increased substantially when tidal forcing is weak or absent (Fig. 3). In those cases, when mixing is comparatively weaker, the persistent upwelling winds, which bring denser water toward the coast (Fig. 1), lead to some stratification, which allows for the development of stronger cross-shelf currents.

The effects of tidal forcing on the cross-shelf circulation along the inner shelf are quantified in Table 1, which shows results of a linear regression analysis of the form $\psi_T = a\psi + b$, where ψ_T and ψ are the tidally averaged offshore transports in the surface layer for simulations forced with and without tides, respectively. Results from the first 10 days of the simulation are used in the analysis. There is a general tendency for the slope of the regression to decrease with increasing tides at all depths shown. At the 20-m isobath, strong tides reduce the tidally averaged transport by 22% compared to the simulation forced by winds only. For weak tides in shallow waters, the slope of the regression is 0.66, and the transports are still highly correlated. During strong tidal forcing, on the other hand, the stratification is further reduced, leading to a virtual shutdown of the cross-shelf circulation (slope = 0.19) compared to when tides are absent (see also Fig. 3, bottom left).

In all cases, the surface transport is approximately equal to the theoretical Ekman transport at large distances from the coast. The reduction in the cross-shelf currents near the coast for increasing tides changes the location and the width of the divergence in the surface transport. The decrease in the stratification due to increased tidal stirring in the shallower regions of the inner shelf extends the region where the cross-shelf circulation is nearly shutdown farther from the coast (Fig. 5, center top). Therefore, the location where the stronger vertical velocity (i.e., the strongest divergence in the surface transport) occurs is moved offshore, effectively increasing the area near the coast sheltered from the influence of offshore waters.

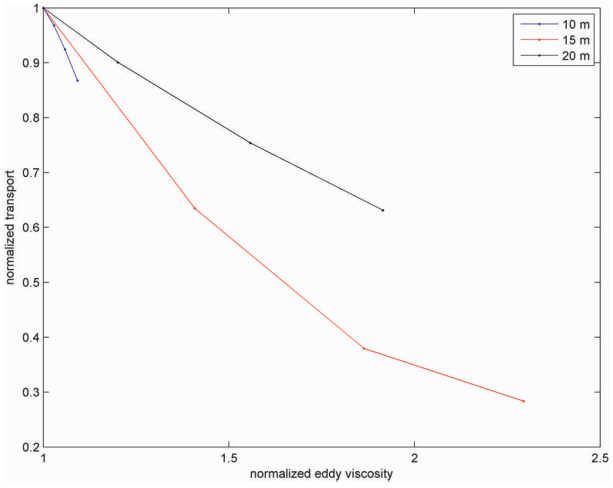

FIG. 4. Normalized cross-shelf transports in the surface layer at 10-, 15-, and 20-m isobaths as a function of normalized eddy viscosity at the middle of the water column for simulations forced by upwelling winds only and by winds and weak, moderate, and strong tides. Values are normalized by the results from the simulation forced by winds only. Values are averaged over one tidal cycle centered on day 3.36.

TABLE 1. Results of a linear regression analysis of the form $\psi_T = a\psi + b$, where ψ_T and ψ are the tidally averaged offshore transports in the surface layer for simulations forced with and without tides, respectively. Results from first 10 days of the simulations are used in the analysis; r is the correlation coefficient between ψ and ψ_T.

h (m)	Weak tides	Moderate tides	Strong tides
10	$r = 0.84$	$r = 0.56$	$r = 0.60$
	$\psi_T = 0.66\psi + 0.01$	$\psi_T = 0.30\psi + 0.02$	$\psi_T = 0.19\psi + 0.02$
15	$r = 0.88$	$r = 0.85$	$r = 0.77$
	$\psi_T = 0.75\psi + 0.07$	$\psi_T = 0.70\psi + 0.05$	$\psi_T = 0.57\psi + 0.06$
20	$r = 0.98$	$r = 0.97$	$r = 0.95$
	$\psi_T = 0.92\psi + 0.01$	$\psi_T = 0.87\psi - 0.01$	$\psi_T = 0.78\psi - 0.01$

Even though the offshore shift is relatively small, it represents a significant fraction of the inner shelf and leads to large changes in water parcel displacement. This is nicely illustrated by comparing the Lagrangian labels [see Eq. (1)] between the simulation forced with no tides and the simulations forced by weak, moderate, and strong tides (Fig. 6). Numbers contoured are distances in kilometers, and negative numbers mean waters come from shallower regions compared with the simulation forced by winds only. As discussed above, the effect of increasing tides is to move the upwelling circulation farther from the coast. As a consequence of that, the near-coastal region does not communicate as efficiently with the offshore area, and waters found there come from much shallower isobaths. The absolute values of the differences are quite significant, with values as high as 40 km along the inner shelf. Note that high values are found even for weak tidal forcing, and that the area with high values increases substantially with increasing tides. Near the 20-m isobath, the difference in displacement is slightly positive, particularly when tides are strong (Fig. 6). Austin and Lentz (2002) showed that, when upwelling winds with no tides are considered in a model setup similar to the one used here, there is a region around the 20-m isobath in the "interior," between the surface and bottom boundary layers (just offshore of where upwelling occurs), that is sheltered from the general cross-shelf circulation (see their Fig. 13, closed contour in the streamfunction panel). If tides are also considered in addition to the winds, the upwelling circulation and this interior region where the streamfunction contours are closed are shifted offshore. As a consequence of that, waters from deeper regions end up reaching the midwater column around the 20-m isobath when tides are considered, explaining the slightly positive values in the difference in the water displacement observed there (Fig. 6).

The reduction in the velocities close to the coast due to increased tides will also affect particle transport on the inner shelf (Fig. 7). For each simulation, drifters were released 1.5–2 m above the bottom at both the 15- and 20-m isobaths (10 and 15 km from the coast, respectively). Drifters first move onshore and then upward following the upwelling circulation before heading offshore. The offshore transport of the drifter released at the 20-m isobath is delayed by one full day (~25% increase)

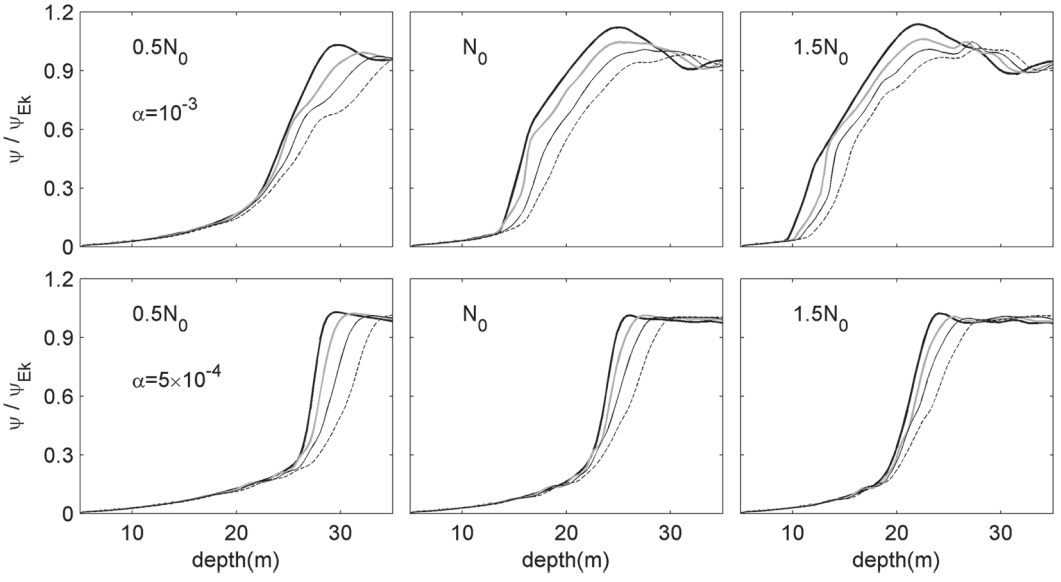

FIG. 5. Cross-shelf transport in the surface layer normalized by theoretical Ekman transport as a function of water depth for simulations forced by upwelling winds only (thick black) and by winds and weak (gray), moderate (thin black), and strong (dashed) tides. Results are averaged over one tidal cycle centered on day 3.36. Results for $\alpha =$ (top) 0.001 and (bottom) 0.0005. Initial stratification increases from left to right.

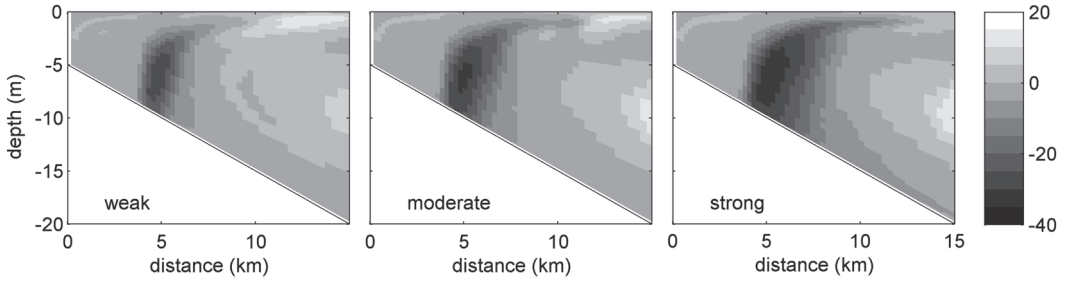

FIG. 6. Difference in water displacement between the simulation forced by upwelling winds only and the simulations forced by winds and weak, moderate, and strong tides [$X_{\text{with\_tide}}(x, z, t)$ minus $X_{\text{no\_tide}}(x, z, t)$; see Eq. (1)] after 6.47 days. Contours are distances in km, and negative numbers mean waters come from shallower regions compared with the simulation forced by winds only.

for the strong tides scenario compared with the simulation forced by winds only. Weaker tidal forcing leads to a smaller but still substantial delay. For drifters released at the 15-m isobath, the effect is much more dramatic. In that case, even weak tides lead to a considerable delay (2 days, ~33% increase) in the offshore movement of the drifter near the surface. For moderate and strong tides, the drifter begins to move offshore at days 10 and 11.5, respectively (not shown). In those cases, the decrease in the cross-shelf transport due to increased mixing is large enough to nearly double the period the drifters remain near the coast.

b. Oscillatory winds

The inner-shelf cross-shelf circulation that developed in response to steady upwelling and downwelling winds is asymmetric (Austin and Lentz 2002). To explore the net effects of this asymmetry, the model is forced by alongshelf winds that oscillate between upwelling and downwelling favorable with a period equal to six inertial periods (~4.7 days). No tides are considered in this simulation. Even though the wind forcing has a zero mean, the offshore transport in the surface layer at the inner shelf does not (Fig. 8). At both the 10- and 15-m

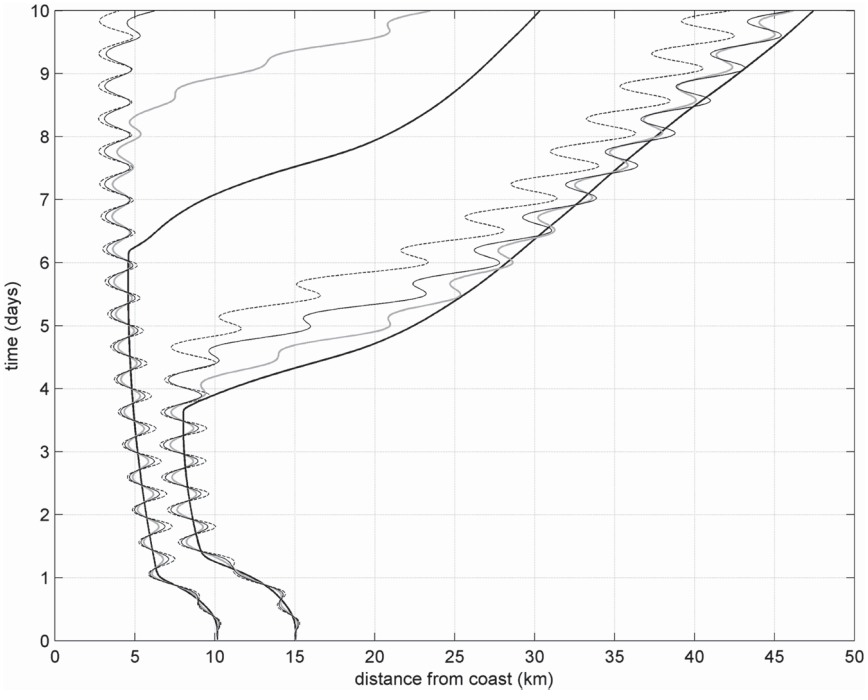

FIG. 7. Drifters trajectories as a function of distance from the coast and time for simulations forced by upwelling winds only (thick black) and by winds and weak (gray), moderate (thin black), and strong (dashed) tides. Drifters were released near the bottom at the 15- and 20-m isobaths (10 and 15 km from the coast, respectively).

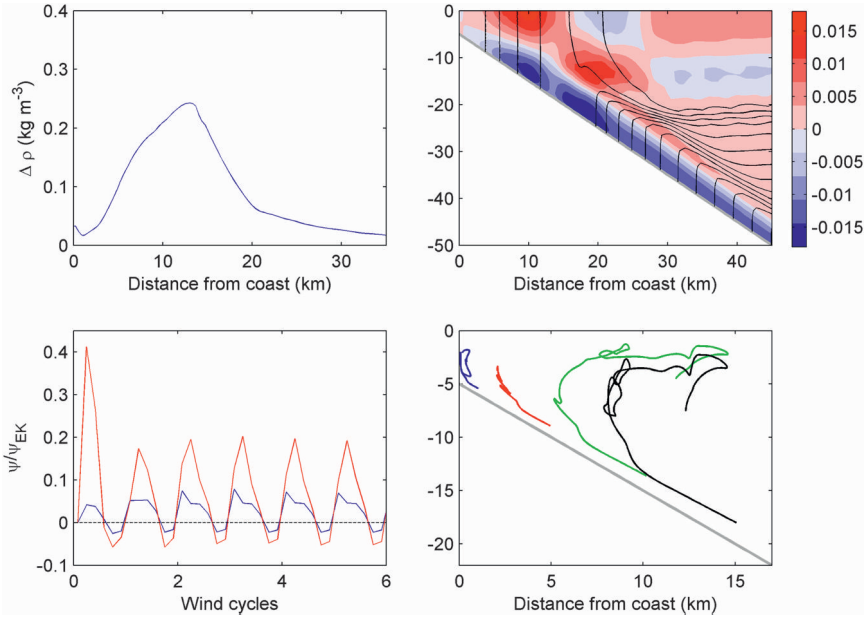

FIG. 8. (top left) Density difference $\Delta\rho$ (ρ after three wind cycles minus initial ρ) and (bottom left) cross-shelf transport in the surface layer normalized by the absolute value of the theoretical Ekman transport at the 10- (blue) and 15- (red) m isobaths. Each wind cycle lasts six inertial periods (~4.7 days). (top right) The cross-shelf velocity (m s^{-1}) averaged over three wind oscillations and the density field at the end of the three oscillations. (bottom right) Drifter trajectories during three wind cycles. Simulation forced by oscillatory winds and $N = N_0$.

isobaths, the surface offshore transport (ψ/ψ_{EK}) during upwelling-favorable winds is much larger than the onshore transport during downwelling-favorable winds. As a consequence of that, the cross-shelf currents at the inner shelf *averaged* over three wind cycles and the density field *at the end* of the three oscillations are biased toward upwelling. This asymmetric response leads to a net increase in the depth-averaged density inshore of about 20 km from the coast, with a peak centered at 10–15 km offshore. Drifters released near the bottom are brought onshore and upward before being transported offshore near the surface, consistently with the averaged cross-shelf velocities. Note that in the offshore region where the boundary layers do not overlap (e.g., 40 km from the coast), the averaged cross-shelf currents are much weaker than over the inner shelf. There, the cross-shelf circulation is nearly symmetric as expected, and the averaged cross-shelf currents are nonzero mostly because the boundary layers grow over time. As the boundary layers grow, the transport between upwelling and downwelling wind cycles is distributed over an increasingly thicker layer, leading to small differences in the velocity magnitude and to a nonzero (but small) average.

The period of the wind oscillation is dynamically relevant for the rectification of the cross-shelf circulation, with larger periods leading to more net upwelling and consequently to larger depth-averaged densities at the inner shelf (Fig. 9, top left). The increase in density is roughly linearly related to the increase in the period for short periods of wind oscillations, tending to level off as the period increases (Fig. 9, top right). Trajectories of drifters released near the bottom show a consistent picture. For winds oscillating at a high frequency, the net displacement is relatively small. As the period of the oscillation increases, however, there is a general tendency for the drifters to be transported following an upwelling circulation. Using $\alpha = 5 \times 10^{-4}$ produces results consistent with this description, although the increase in the depth-averaged density on the inner shelf is somewhat smaller.

The strength of the vertical stratification is also important in the rectification process. Although the response during downwelling winds is similar to before, with the inner shelf quickly becoming nearly homogeneous in the vertical, a stronger stratification allows for a larger flux of dense water toward the coast during upwelling-favorable winds, which leads to a stronger asymmetry in the response. The cross-shelf currents in the shallow regions averaged over three wind cycles are stronger than before, as is the increase in the depth-averaged density near the coast (Fig. 10). A decrease in the stratification has an opposite effect (Fig. 11), leading to less rectification. Note that the offshore transport in the surface layer at the 10-m isobath is nearly symmetric

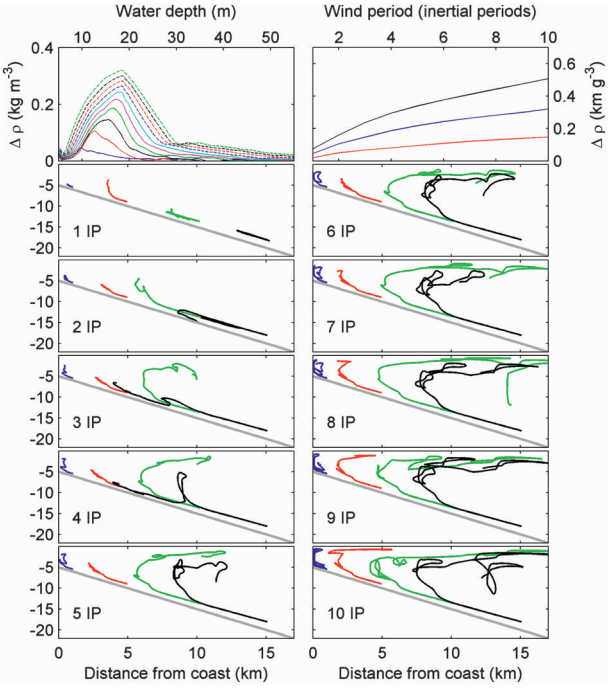

FIG. 9. (top) Density difference $\Delta\rho$ (ρ after three wind cycles minus initial ρ) for simulations forced by winds oscillating with different periods, ranging from 1 (solid blue) to 10 (dashed green) inertial periods (IPs). (bottom) Drifter trajectories during three wind cycles. (top right) Maximum density difference at the inner shelf after three wind cycles for different periods of wind oscillation for $N = 0.5N_0$ (red), $N = N_0$ (blue), and $N = 1.5N_0$ (black).

for the low-stratification case. Before, when stratification was stronger, the increased mixing due to the upwelling wind pulse was not enough to completely mix the water column, and the remaining stratification allowed for a cross-shelf circulation to be established, which brought denser water toward the coast. If the stratification is too weak (Fig. 11), however, the wind mixing homogenizes the shallower regions of the inner shelf, leading to a shutdown of the transport during the upwelling phase too (cf. ψ/ψ_{EK} time series between Figs. 10 and 11). With no rectification near the 10-m isobath (5 km from the coast), the depth-averaged density increases only slightly there (Fig. 11). Offshore, however, where the stratification is not completely destroyed by wind mixing, the asymmetric response is observed. There is a more substantial increase in the depth-average density, and the drifter trajectory is consistent with an upwelling circulation.

The inclusion of tidal forcing leads to a decrease in the rectification of the cross-shelf circulation (Fig. 12). There is a ~30% reduction in the increase of the depth-averaged density on the inner shelf for the strong tidal forcing case (compared to the no-tides case), and a drifter released near the bottom at the 15-m isobath ends up trapped in a region of low cross-shelf currents near the coast. Weaker tidal forcing also affects the rectification, but to a lesser degree.

4. Discussion and conclusions

The comparison of results from a simulation where the coastal ocean is forced by upwelling-favorable alongshore winds with no tides with results from simulations forced by tidal currents of different intensities in addition to the wind reveals that the tidally averaged cross-shelf circulation over the inner shelf is substantially modified by tides. In general, under upwelling-favorable wind forcing, stronger tides lead to lighter waters close to the coast (Fig. 1). This can be at least partially explained by the fact that tidal stirring near the bottom in the offshore region will lead to a decrease in the water density in the bottom boundary layer, as the heavier water near the bottom is mixed with lighter water from above. As a consequence of that, lighter water is advected by the upwelling circulation toward the coast when tides are present compared to the simulation forced by winds only. However, this description does not provide a complete picture of the process. Analyses using Lagrangian labels (as in Kuebel Cervantes et al. 2003) indicate that water parcel displacement is substantially modified as tidal forcing increases (Fig. 6). Previous studies of inner-shelf circulation have revealed a strong relationship between stratification, eddy viscosity profiles, and wind-driven cross-shelf circulation (e.g., Lentz 1995, 2001; Austin and Lentz 2002; Kirincich et al. 2005). As tidal currents increase, there is a tendency for increased mixing, larger eddy viscosity coefficients (Fig. 2), and reduced stratification along the inner shelf. As a consequence of that, tidally averaged cross-shelf currents are weaker (Fig. 3), leading to substantial reduction in the transport of deep, dense waters toward the coast (Fig. 6). Although changes in the bottom stress due to tides may contribute to the observed changes in the cross-shelf circulation on the inner shelf, results suggest that the enhanced mixing throughout the water column plays a dominant role (Fig. 4). The residual circulation due to tides only is at least one order of magnitude smaller than the tidally averaged wind-driven flow, suggesting that tidal residual currents do not play a crucial role modifying the cross-shelf circulation.

Key aspects affecting the importance of tides on the wind-driven cross shelf circulation are the bottom slope and the strength of the stratification. A stronger initial stratification (Fig. 5, right) generally allows the upwelling circulation to reach closer to the coast, while weaker initial stratification (Fig. 5, left) moves the location of stronger vertical velocities offshore, which is consistent with Lentz's (2001) observations. Tidal effects seem equally important for both bottom slopes used. Note that the shift in the

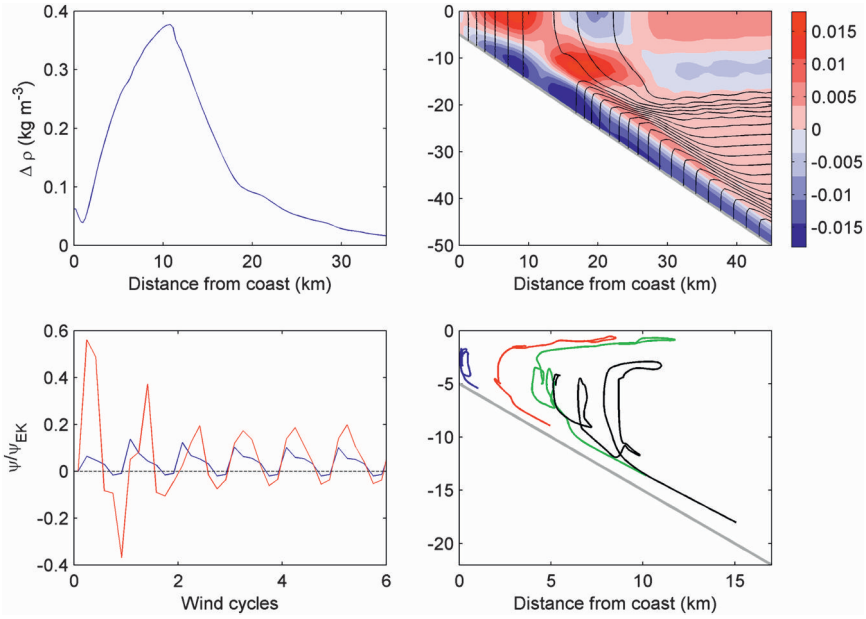

FIG. 10. Same as in Fig. 8, but for $N = 1.5N_0$.

upwelling circulation caused by increasing the tidal forcing for a given stratification (the process investigated in this study) is just as large as the shift caused by substantially changing the stratification for a given observed tidal forcing [the process reported by Lentz (2001)].

The weaker subtidal cross-shelf circulation along the inner shelf due to tides leads to large changes in particle displacement patterns (Fig. 7). Drifters' trajectories indicate that, even for weak tides, alongshore upwelling-favorable winds may need to blow for long time periods (8–12 days) for particles to be advected offshore. This increase in residence time near the coast occurs because the upwelling circulation is shifted offshore in response to increased mixing near the coast (Fig. 5), effectively isolating waters near the coast from waters offshore. The increase in residence time can be quite substantial, as quantified by releasing a passive tracer in the simulations. The initial dye concentration for all cases is set to one inshore of the 15-m isobath, and to zero offshore. If no tides are considered, the upwelling circulation

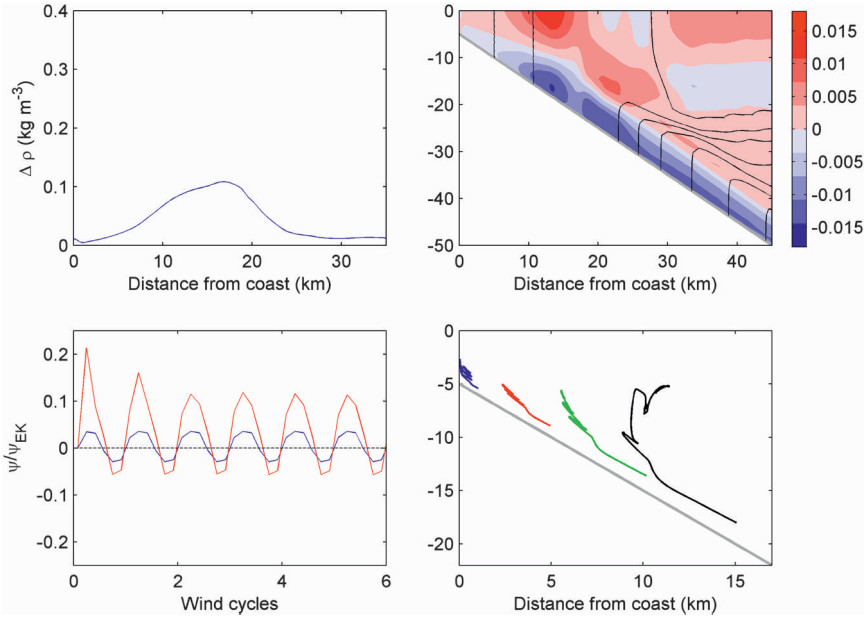

FIG. 11. Same as in Fig. 8, but for $N = 0.5N_0$.

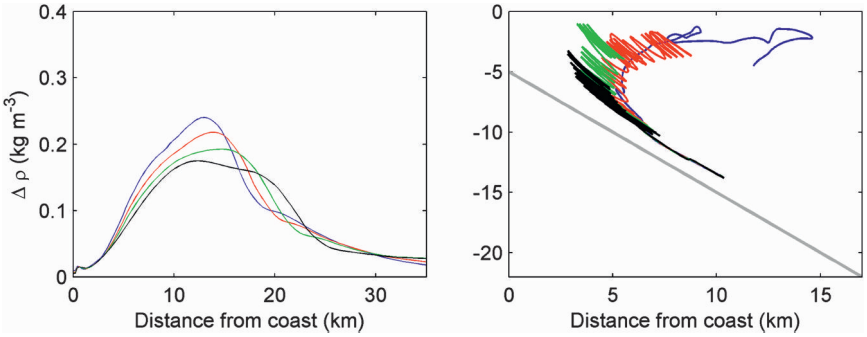

FIG. 12. (left) Density difference $\Delta\rho$ (ρ after three wind cycles minus initial ρ) for the simulation forced by oscillatory winds only (blue) and oscillatory winds and weak (red), moderate (green), and strong (black) tides. (right) Drifter trajectories during three wind cycles; $N = N_0$.

reduces the total amount of dye inshore of the 15-m isobath by 30% in 4.7 days, and by half in 9 days (Table 2). Weak, moderate, and strong tidal forcings increase the residence times by approximately 16%–28%, 37%–44%, and 61%–70%, respectively.

The substantial changes in residence time near the coast and at the source of the upwelled water will have important ecosystem implications. Since upwelled waters come from much shallower regions when tides are strong, the flux of cold, dense, nutrient-rich waters toward the coast will presumably be reduced, potentially affecting nearshore biological processes. Species that prefer to remain near the coast at some stage of their life cycle, however, may find environments with stronger tides beneficial. In this study, only the M_2 tidal constituent was considered for simplicity. However, since the primary effect of the tidal currents in this process is to increase mixing, we expect a similar effect for other constituents. In regions where there is large variability in the intensity of the tidal currents during the spring–neap cycle, the efficiency of the wind to drive cross-shelf currents and the flux of nutrients toward the coast for a given wind stress may be modulated by that cycle.

It is interesting to note that in Kuebel Cervantes et al.'s (2003) numerical simulations the standard deviation of the temperature field during summer in waters shallower than 10 m was higher than the observed variability both in moorings and in shipboard surveys (see their Fig. 5). The simulations did not consider tidal forcing, and upwelling occurred very near the coast, on average inshore of the 10-m isobath (see summer mean streamfunction plot in their Fig. 6). The inclusion of tidal forcing in the model would lead to upwelling occurring farther offshore, potentially decreasing the temperature variability close to the coast and bringing the model simulations closer to the observations.

It is also important to point out that, even though only barotropic tides were considered in these simulations, internal gravity waves (IGWs) also have significant signatures on the shelf (Denbo and Allen 1984). Avicola et al. (2007) used observations from the Oregon coast to show that baroclinic velocities associated with IGWs of M_2 frequency can play a major role in enhancing the vertical shear. Their analyses reveal a striking correspondence of sheets of elevated turbulence dissipation rate with regions of low IGW-derived Richardson numbers, and led them to conclude that midwater turbulence generation in that dataset required the IGW field to provide the necessary shear. The inclusion of an IGW field at M_2 or near f frequency in the model would presumably enhance the effects observed in the present simulations, with an even larger shift in the location where the strongest divergence in the surface transport occurs. This is an important practical limitation, since most coastal models do not include IGWs properly (Avicola et al. 2007).

Austin and Lentz's (2002) results reveal that the situation during downwelling-favorable wind stress is quite different than during upwelling winds. The cross-shelf circulation induced by downwelling winds in a stratified shelf forces surface, light water under near-bottom, dense waters. This leads to convection, substantially increasing mixing and resulting in a vertically homogeneous inner shelf and the shutdown of the cross-shelf circulation (see their Figs. 3 and 13). Since the water column is already homogenized, the inclusion of tidal forcing produces no

TABLE 2. Residence time at the inner shelf, computed as the time necessary for the total amount of dye inshore of the 15-m isobath to decrease to 70% (T_{70}) or to 50% (T_{50}) of the initial value. Initial dye concentration is set to 1 inshore of the 15-m isobath, and to 0 offshore.

	No tides	Weak	Moderate	Strong
T_{70} (days)	4.68	5.97	6.74	7.97
T_{50} (days)	8.95	10.35	12.23	14.41

notable effect on the wind-driven cross-shelf circulation on the inner shelf. The effects of tides on the subtidal inner-shelf circulation are only significant during upwelling-favorable wind forcing.

This asymmetry in the response of the inner shelf to upwelling–downwelling wind forcing can lead to a rectification of the cross-shelf circulation. The rectification occurs because the cross-shelf transport is nonzero during upwelling wind forcing, when the inner shelf is stratified, but is approximately zero during downwelling winds, when the inner shelf is nearly unstratified. Therefore, the cross-shelf circulation at the inner shelf averaged over a period when the wind oscillates between upwelling and downwelling favorable with zero mean is biased toward an upwelling circulation (Fig. 8), establishing a net flux of potentially nutrient-rich waters into the inner shelf that could fuel biological activity. The rectification increases with increasing shelf stratification (Figs. 8, 10, and 11), when the flux of dense water toward the inner shelf under upwelling-favorable winds is largest. The period of the wind oscillation is also important, with larger periods leading to more intense net upwelling (Fig. 9).

The rectification of the cross-shelf circulation is most likely to be important in regions characterized by weak tidal forcing. As discussed before, tides will increase mixing and decrease the cross-shelf circulation near the coast during upwelling winds (Figs. 2–5), but will have a negligible effect during downwelling wind forcing. Therefore, tides can substantially reduce the asymmetric response of the cross-shelf circulation at the inner shelf to upwelling–downwelling wind cycles, reducing the potential for rectification (Fig. 12).

The vertical structure of the stratification, in addition to its strength, is very important for the cross-shelf circulation developed in response to tidal forcing and oscillatory winds. In the majority of Austin and Lentz's (2002) numerical simulations, the initial stratification consisted of well-mixed surface and bottom layers with a continuously stratified pycnocline in between. In that case, upwelling winds cause the pycnocline to outcrop and move offshore, after which the inner shelf is fed by a body of constant-density water. As a result, the stratification on the inner shelf is very weak. If the initial stratification is constant (as in our simulations), however, upwelling winds lead to a constant supply of increasingly denser water to the inner shelf, resulting in stronger stratification (Austin and Lentz 2002; cf. their Figs. 2 and 13). In a two-layer system, the effects of tidal forcing on the wind-driven cross-shelf circulation will be reduced compared to those in the constant-stratification scenario. This is because the water column over the shallow waters in a two-layer system is already nearly vertically homogeneous after the pycnocline outcrop, even in the absence of tides. The rectification is response to oscillatory winds will also be reduced. Even though the east coast of the United States is generally characterized as a strongly two-layered shelf, observations collected along the Rutgers University Glider Endurance Line (Castelao et al. 2008) off central New Jersey indicate that there are several instances when the shelf presents a nearly constant stratification (Fig. 13). Note that the observations span several months over different years. There are also times when the shelf-wide density structure is similar to a two-layer system, but the region within 30 km from the coast remains linearly stratified (Fig. 13, bottom). A near-bottom density gradient exists in those cases, so upwelling winds would provide a supply of continuously denser water to the inner shelf as in the simulations initialized with constant stratification. Other examples in which the region close to the coast on the Middle Atlantic Bight presents a nearly constant stratification

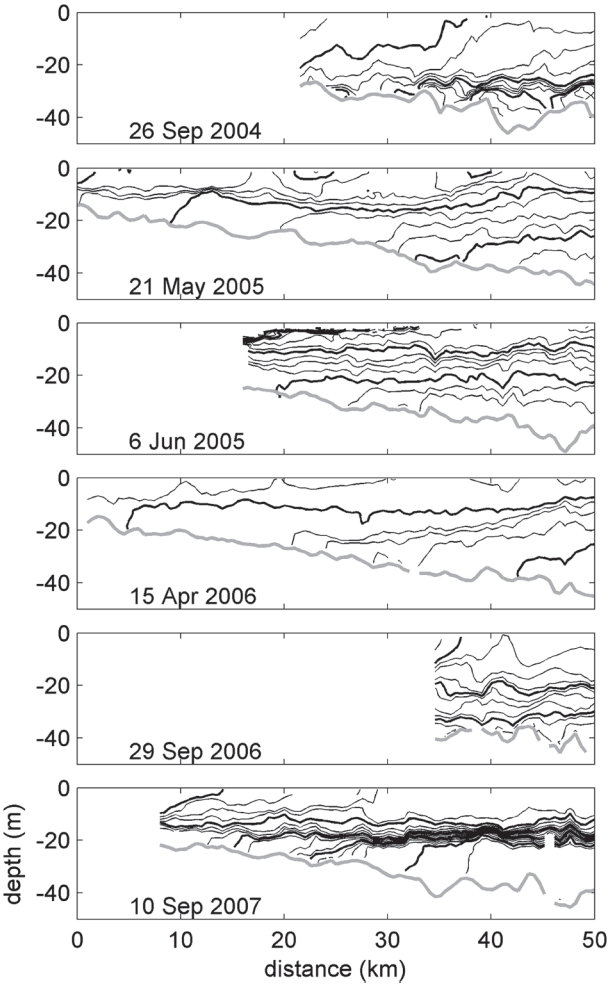

FIG. 13. Density cross-shelf sections along the Rutgers University Glider Endurance Line off NJ. Contour interval is 0.25 kg m^{-3}, with boldface contours every 1 kg m^{-3}.

can be found in Yankovsky et al. (2000, their Fig. 13), Münchow and Chant (2000, their Fig. 3), and Glenn et al. (2004, their Fig. 5). Münchow and Chant (2000), in particular, present time series of temperature at the 12-m isobath (mooring C1; their Fig. 3) spanning an 80-day period from mid-May to early August. The thermistor chain observations indicate that the water column is very rarely vertically homogeneous; most of the times the water column is stratified. Even more interestingly, their observations indicate that, during a 12-day upwelling wind event (days 158–170), bottom waters cooled by more than 5°C at an approximately constant rate. Therefore, even during this very persistent upwelling event on the Middle Atlantic Bight, a nearly constant supply of denser waters toward the coast was observed, demonstrating the relevance of using an initially constant stratification in the present study.

In all simulations, the wind forcing was aligned with the coastline. Previous studies have shown that the cross-shelf component of the wind can play a very significant role in driving cross-shelf currents on the inner shelf (Tilburg 2003; Fewings et al. 2008). However, those studies have shown that the overturning circulation generated as a result of cross-shelf wind forcing is located above the pycnocline. Therefore, since the return flow is located mostly on the surface mixed layer, there will not be a continuous supply of dense waters to the inner shelf and, presumably, the processes discussed here will not be substantial.

Lastly, the current model implementation presents the obvious limitation of being two-dimensional. In the real ocean, three-dimensional effects are important most of the time. Interactions with topographic features, the intrusion of buoyancy currents, the establishment of alongshore pressure gradients, and other process will affect the cross-shelf circulation. Using a two-dimensional model, however, greatly simplifies the problem and makes it much easier to isolate the cause and effect. It also allows for comparison with other recent studies that used a two-dimensional setup (Austin and Lentz 2002; Kuebel Cervantes et al. 2003; Tilburg 2003; Lentz and Chapman 2004).

In conclusion, the numerical simulations indicate that tidal forcing and oscillatory winds can substantially affect the subtidal cross-shelf circulation over the inner shelf. Tidal currents lead to increased mixing, reduced stratification, and consequently to a reduction in the efficiency of the winds to drive cross-shelf currents over the shallow regions. The upwelling circulation is shifted offshore, increasing the residence time near the coast and changing the displacement of water parcels over the shallow regions. Due to the asymmetric response of the inner shelf to upwelling–downwelling wind forcing, fluctuating winds with zero mean lead to a rectification of the cross-shelf circulation and net upwelling, with potentially important ecosystem implications. The rectification increases for stronger stratification and when winds fluctuate at low frequencies.

Acknowledgments. We gratefully acknowledge support by the Office of Naval Research (Grant N000140610739) and by the National Science Foundation (Grant OCE 0238957).

REFERENCES

Allen, J., 1980: Models of wind driven currents on the continental shelf. *Annu. Rev. Fluid Mech.,* **12,** 389–433.

——, P. Newberger, and J. Federiuk, 1995: Upwelling circulation on the Oregon continental shelf. Part I: Response to idealized forcing. *J. Phys. Oceanogr.,* **25,** 1843–1866.

Austin, J., and S. Lentz, 2002: The inner shelf response to wind-driven upwelling and downwelling. *J. Phys. Oceanogr.,* **32,** 2171–2193.

Avicola, G. S., J. N. Moum, A. Perlin, and M. D. Levine, 2007: Enhanced turbulence due to the superposition of internal gravity waves and a coastal upwelling jet. *J. Geophys. Res.,* **112,** C06024, doi:10.1029/2006JC003831.

Battisti, D., and A. Clarke, 1982: A simple method for estimating barotropic tidal currents on continental margins with specific application to the M_2 tide off the Atlantic and Pacific coasts of the United States. *J. Phys. Oceanogr.,* **12,** 8–16.

Castelao, R. M., S. Glenn, O. Schofield, R. Chant, J. Wilkin, and J. Kohut, 2008: Seasonal evolution of hydrographic fields in the central Middle Atlantic Bight from glider observations. *Geophys. Res. Lett.,* **35,** L03617, doi:10.1029/2007GL032335.

Chapman, D. C., 1985: Numerical treatment of across-shore open boundaries in a barotropic ocean model. *J. Phys. Oceanogr.,* **15,** 1060–1075.

Denbo, D. W., and J. S. Allen, 1984: Rotary empirical orthogonal function analysis of currents near the Oregon coast. *J. Phys. Oceanogr.,* **14,** 35–46.

Ekman, V., 1905: On the influence of the Earth's rotation on ocean currents. *Ark. Math. Astro. Fys.,* **2,** 1–53.

Fewings, M., S. Lentz, and J. Fredericks, 2008: Observations of cross-shelf flow driven by cross-shelf winds on the inner continental shelf. *J. Phys. Oceanogr.,* **38,** 2358–2378.

Flather, R., 1976: A tidal model of the northwest European continental shelf. *Mem. Soc. Roy. Sci. Liege,* **6,** 141–164.

Galperin, B., L. Kantha, S. Hassid, and A. Rosati, 1988: A quasi-equilibrium turbulent energy model for geophysical flows. *J. Atmos. Sci.,* **45,** 55–62.

Garrett, C., J. Keeley, and D. Greenberg, 1978: Tidal mixing versus thermal stratification in the Bay of Fundy and Gulf of Maine. *Atmos.–Ocean,* **16,** 403–423.

Glenn, S., and Coauthors, 2004: Biogeochemical impact of summertime coastal upwelling on the New Jersey Shelf. *J. Geophys. Res.,* **109,** C12S02, doi:10.1029/2003JC002265.

Haidvogel, D. B., and Coauthors, 2008: Regional ocean forecasting in terrain-following coordinates: Model formulation and skill assessment. *J. Comput. Phys.,* **227,** 3595–3624.

He, R., and J. Wilkin, 2006: Barotropic tides on the southeast New England shelf: A view from a hybrid data assimilative modeling approach. *J. Geophys. Res.,* **111,** C08002, doi:10.1029/2005JC003254.

Huyer, A., 1990: Shelf circulation. *The Sea,* B. LeMehaute and D. M. Hanes, Eds., Ocean Engineering Science, Vol. 9A, John Wiley and Sons, 1647–1658.

Kirincich, A., J. Barth, B. Grantham, B. Menge, and J. Lubchenco, 2005: Wind-driven inner-shelf circulation off central Oregon during summer. *J. Geophys. Res.,* **110,** C10S03, doi:10.1029/2004JC002611.

Kuebel Cervantes, B., and J. Allen, 2006: Numerical model simulations of continental shelf flows off northern California. *Deep-Sea Res. II,* **53,** 2956–2984.

——, ——, and R. Samelson, 2003: A modeling study of Eulerian and Lagrangian aspects of shelf circulation off Duck, North Carolina. *J. Phys. Oceanogr.,* **33,** 2070–2092.

Lentz, S., 1995: Sensitivity of the inner-shelf circulation to the form of the eddy viscosity profile. *J. Phys. Oceanogr.,* **25,** 19–28.

——, 2001: The influence of stratification on the wind-driven cross-shelf circulation over the North Carolina shelf. *J. Phys. Oceanogr.,* **31,** 2749–2760.

——, and D. Chapman, 2004: The importance of nonlinear cross-shelf momentum flux during wind-driven coastal upwelling. *J. Phys. Oceanogr.,* **34,** 2444–2457.

Limeburner, R., and R. Beardsley, 1982: The seasonal hydrography and circulation over Nantucket Shoals. *J. Mar. Res.,* **40,** 371–406.

Marchesiello, P., J. C. McWilliams, and A. Shchepetkin, 2001: Open boundary conditions for long-term integration of regional oceanic models. *Ocean Modell.,* **3,** 1–20.

Mellor, G., and T. Yamada, 1982: Development of a turbulence closure model for geophysical fluid problems. *Rev. Geophys. Space Phys.,* **20,** 851–875.

Münchow, A., and R. J. Chant, 2000: Kinematics of inner shelf motion during the summer stratified season off New Jersey. *J. Phys. Oceanogr.,* **30,** 247–268.

Shchepetkin, A. F., and J. C. McWilliams, 1998: Quasi-monotone advection schemes based on explicit locally adaptive diffusion. *Mon. Wea. Rev.,* **126,** 1541–1580.

——, and J. McWilliams, 2003: A method for computing horizontal pressure-gradient force in an oceanic model with a nonaligned vertical coordinate. *J. Geophys. Res.,* **108,** 3090, doi:10.1029/2001JC001047.

——, and ——, 2005: The Regional Oceanic Modeling System (ROMS): A split-explicit, free-surface, topography-following-coordinate oceanic model. *Ocean Modell.,* **9,** 347–404.

Simpson, J., and J. Hunter, 1974: Fronts in the Irish Sea. *Nature,* **250,** 404–406.

——, C. Allen, and N. Morris, 1978: Fronts on the continental shelf. *J. Geophys. Res.,* **83,** 4607–4614.

Smith, R., 1995: The physical processes of coastal ocean upwelling systems. *Upwelling and the Ocean: Modern Processes and Ancient Records,* C. P. Summerhayes et al., Eds., John Wiley and Sons, 39–64.

Tilburg, C., 2003: Across-shelf transport on a continental shelf: Do across-shelf winds matter? *J. Phys. Oceanogr.,* **33,** 2675–2688.

Wilkin, J., 2006: The summertime heat budget and circulation of southeast New England shelf waters. *J. Phys. Oceanogr.,* **36,** 1997–2001.

Yankovsky, A. E., R. W. Garvine, and A. Münchow, 2000: Mesoscale currents on the inner New Jersey shelf driven by the interaction of buoyancy and wind forcing. *J. Phys. Oceanogr.,* **30,** 2214–2230.